

Title	Effect of the crystallization-induction layer of yttria-stabilized zirconia on the solid state crystallization of an amorphous Si film
Author(s)	Horita, Susumu; Akahori, Tetsuya
Citation	Japanese Journal of Applied Physics, 53(3): 030303-1-030303-4
Issue Date	2014-01-31
Type	Journal Article
Text version	author
URL	http://hdl.handle.net/10119/11939
Rights	This is the author's version of the work. It is posted here by permission of The Japan Society of Applied Physics. Copyright (C) 2014 The Japan Society of Applied Physics. Susumu Horita and Tetsuya Akahori, Japanese Journal of Applied Physics, 53(3), 2014, 030303-1-030303-4. http://dx.doi.org/10.7567/JJAP.53.030303
Description	

1 **Effect of the Crystallization-Induction Layer of Yttria-Stabilized**
2 **Zirconia on the Solid State Crystallization of an Amorphous Si Film**

3
4 Susumu Horita* and Tetsuya Akahori

5 School of Materials Science, Japan Advanced Institute of Science and Technology,

6 Nomi, Ishikawa 923 – 1292, Japan

7 E-mail: horita@jaist.ac.jp

8
9 **Abstract**

10 We investigated the crystallization-induction (CI) effect of yttria-stabilized zirconia
11 (YSZ) on the solid phase crystallization of amorphous Si (a-Si) films. The incubation
12 time τ_i for crystallization on a polycrystalline YSZ layer was shorter than that on a glass
13 substrate. From the result of Arrhenius plots of $1/\tau_i$, it is suggested that the CI effect is
14 not due to the difference in the activation energy E_i but to a higher nucleation site area
15 density on the YSZ layer. Also, preheating the YSZ layer prior to a-Si film deposition
16 was effective to shorten the incubation time τ_i because E_i was reduced.

1 Polycrystalline silicon (poly-Si) TFTs have great advantages of higher stability or
2 reliability and higher mobility. Since the demands for applications of poly-Si TFTs are
3 low-temperature fabrication, low cost, and high performance, several methods to
4 fabricate poly-Si films have been proposed, such as solid phase crystallization (SPC),^{1,2)}
5 metal-induced crystallization (MIC),^{3,4)} metal-induced lateral crystallization (MILC),^{5,6)}
6 pulse laser annealing (PLA)⁷⁻⁹⁾, etc.^{10,11)} However, each individual method has some
7 drawbacks such as a high process temperature, a long annealing time, remnant metal as
8 a leakage current source, non-uniform device performance, and so on.

9 So far, in order to obtain a poly-Si film with a uniform electrical property in
10 fabrication conditions of both a short time and low temperature, we have proposed a
11 crystallization-induction (CI) layer method using yttria-stabilized zirconia
12 $[(\text{ZrO}_2)_{1-x}(\text{Y}_2\text{O}_3)_x : \text{YSZ}]$ as a CI material.^{12,13)} In this method, an amorphous Si (a-Si)
13 film is deposited on a YSZ layer that covers the surface of a substrate. Since YSZ has a
14 small lattice mismatch of $\sim 5\%$ and the same cubic crystal structure as Si, it can be
15 expected that a poly-Si film thus obtained has a uniform grain size and crystallographic
16 orientation, owing to crystallographic information of the YSZ layer. Actually, we
17 produced a crystallized Si film by directly depositing on a polycrystalline YSZ
18 (poly-YSZ) layer at the substrate temperature of $320\text{ }^\circ\text{C}$, which was $\sim 100\text{ }^\circ\text{C}$ lower than
19 that on the glass substrate without the YSZ layer.¹³⁾ However, the surface of directly
20 deposited poly-Si films is generally much rough, compared with SPC poly-Si films.¹⁾ So,
21 for a reduction of the surface roughness of crystallized Si films, we tried to crystallize
22 an a-Si film in the solid phase on a poly-YSZ layer by furnace annealing.

23 In this study, we focus on the CI effect of the poly-YSZ layer on the SPC of a-Si film
24 and investigate it, and the results are compared to those obtained with a glass substrate

1 without the YSZ layer and a single crystal (111)-oriented YSZ substrate as an
2 underlying substance. Since the cleanness of a deposition surface is important for Si
3 film growth on it, we also tried to heat a poly-YSZ layer in a deposition vacuum
4 chamber just before Si film deposition, in order to remove out contaminants absorbed
5 on the sample during loading. Hereafter, this heating process is called preheating. In the
6 paper, we present the investigation results and discuss them, in particular, from the
7 viewpoints of thermodynamic activation energy and nucleation density of the CI layer
8 of the YSZ.

9 Figure 1 shows the schematic diagrams of the three kinds of sample structures, (a)
10 a-Si film deposited on a poly-YSZ film which covers the surface of a fused quartz
11 substrate (Si/poly-YSZ/glass), (b) a-Si film deposited on a single crystal (111)-oriented
12 YSZ substrate (Si/(111)-YSZ), and (c) a-Si film deposited on a fused quartz substrate
13 (Si/glass). A fused quartz glass substrate ($10 \times 20 \text{ mm}^2$) is chemically cleaned before
14 deposition of a poly-YSZ layer at a substrate temperature of $50 \text{ }^\circ\text{C}$ by reactive
15 magnetron sputtering. Ar and O_2 are used as sputtering and reactive gases, respectively,
16 with a sputtering pressure of $\sim 6.5 \text{ mTorr}$.¹⁴⁾ By X-ray diffraction measurement, it is
17 found that the YSZ layer is preferentially (111)-oriented. This is a main reason why the
18 orientation of the single YSZ substrate is (111). The chemical composition of Y/(Zr+Y),
19 R_Y , in the deposited YSZ layer is estimated to be about 19% by X-ray photoelectron
20 spectroscopy measurement. Before deposition of an Si film, the YSZ layer is chemically
21 cleaned, using a procedure described in the previous report.¹³⁾ Then, a 60-nm-thick a-Si
22 film is deposited on a YSZ/glass substrate with an e-beam evaporation method at $300 \text{ }^\circ\text{C}$
23 at a pressure less than $2 \times 10^{-8} \text{ Torr}$. For comparison, a-Si films are deposited directly on
24 a single (111)-oriented YSZ substrate with an R_Y of 23 % and a glass substrate without

1 YSZ layer, individually. Also, just prior to Si film deposition, some of the
2 poly-YSZ/glass samples are heated at 500 °C for 10 or 60 min in the Si deposition
3 chamber at around the deposition pressure. Subsequently, crystallization of a-Si film is
4 performed by annealing in an electric furnace at a temperature T_A of 560, 570, or 580 °C
5 in a N₂ atmosphere. The crystallization degree of Si films is estimated by Raman
6 spectroscopy using a He-Ne laser beam (632.8 nm). The crystalline fraction, X_c , is
7 determined by the empirical expression $X_c = (I_c + I_m)/(I_c + I_m + \sigma I_a)$, where I_c , I_m , and I_a
8 are the integrated intensities corresponding to crystalline, intermediate, and amorphous
9 component peaks, respectively, and σ is the ratio of the integrated Raman cross section
10 for the amorphous phase to that for crystalline phase. In this study, σ is chosen to be 1
11 for simplicity.^{15,16)} Depth profiles of Zr and Y in a crystallized Si film are measured by
12 secondary ion mass spectrometry (SIMS).

13 Figures 2 (a), (b), and (c) show the Raman spectra for the three kinds of samples,
14 where the annealing time is a parameter. In Fig. 2(b), a broad and large peak around 600
15 cm⁻¹ is due to the single crystalline substrate of (111)-YSZ. As can be seen from Figs. 2
16 (a) and (b), small Si peaks appear at ~520 cm⁻¹ due to crystalline Si (c-Si) at the
17 annealing time t_a of 775 min. However, in Fig. 2 (c), without the YSZ layer, there is no
18 c-Si peak at the same t_a but, after $t_a = 1000$ min, a small peak of c-Si is observed. This
19 indicates that a-Si films on YSZ crystallize more quickly than without YSZ, probably
20 because of the CI effect of YSZ. After an annealing of about 1000 min, the
21 crystallization shows a saturation tendency, except for (c) without YSZ.

22 Figure 3 shows the annealing time dependences of crystalline fractions X_c of the Si
23 films deposited on a poly-YSZ layer (closed circle), a single (111)-YSZ substrate
24 (cross), and a glass substrate (closed triangle) without preheating. Also, the X_c of an Si

1 /poly-YSZ/glass with preheating (open circle) is shown. As a reference, the broken line
2 indicates the X_c of the Si film annealed at 700 °C for 30 min on a (111)-YSZ substrate.
3 The X_c of ~80% is considered to be an upper-limit value for our sample structures. At
4 first, the non-preheating cases are mentioned. It can be seen that a retardation period or
5 so-called incubation time τ_i before the beginning of the crystallization, and the
6 crystallization rate $R_C = \Delta X_c / \Delta t_a$ of the Si/poly-YSZ/glass case are almost the same as
7 those in the Si/(111)-YSZ case. Here, τ_i is defined by an intercepting time t_a between the
8 horizontal axis and the initial linear line of the crystalline fraction. The τ_i is also a kind
9 of transition time which is necessary to detect a continuous crystallization phenomenon
10 by Raman spectroscopy. Both of $X_{c,s}$ for Si on YSZ increase linearly with the annealing
11 time t_a as a whole. In contrast to this, the beginning of crystallization of the Si/glass is
12 delayed by ~300 min and seems to increase non-linearly with t_a . From this result, we
13 can consider the following growth model.

14 The location of nucleation may be at the interface, according to many other
15 reports^{17,18)}, in which nucleation in an a-Si film occurs at the interface faster than in the
16 bulk. But bulk nucleation cannot be excluded. Also, it is well known that, for bulk
17 nucleation, an initial crystalline fraction varies as the fourth power of the annealing time,
18 based on the assumptions that nucleation occurs randomly at a constant rate and that
19 crystallization proceeds isotropically in direction and linearly in time.¹⁹⁾ On the other
20 hand, if the nucleation occurs at the interface uniformly like a sheet, the crystallization
21 front would go straight toward the film surface linearly with the annealing time so that
22 the X_c should increase as well. This phenomenon has been already reported by other
23 researchers.^{20,21)} In the Si/poly-YSZ/glass and Si/(111)-YSZ cases, Si nucleation is
24 induced at the YSZ interface, and Si-crystallized areas grown from the nucleation sites

1 cover the YSZ interface more uniformly, compared with the Si/glass case. Later, we
2 discuss further this nucleation event. Then, the crystallization front progresses with time
3 linearly toward the film surface. On the contrary, in the Si/glass case, Si nucleation at
4 the interface of SiO₂ may occur non-uniformly in time and space more than in the
5 former cases. Although the initial nucleation site might not be in bulk, the possibility of
6 bulk nucleation increases with the annealing time. For example, at $t_a \approx 1000$ min, bulk
7 nucleation might occur so that the X_c increases rapidly with t_a , as shown in Fig.3.

8 The X_c saturation values in all of the cases are relatively low as a whole, and even
9 in the case of Si/(111)-YSZ, it is less than 80%. These smaller X_c s can be explained by
10 the dependence of the integrated Raman cross section σ on the grain size.^{22,23)} The
11 related issue has been already discussed in our previous paper.¹³⁾ The saturation value
12 decreases in the order of Si/(111)-YSZ, Si/poly-YSZ/glass, and Si/glass, which seems to
13 be due to the dependence on the crystallographic information quality of the underlying
14 substance. For example, the highest value for the Si/(111)-YSZ can be due to an almost
15 perfect information of single (111)-YSZ. However, for further discussion on this, we do
16 not have any clear evidence such as the crystallographic orientation, the grain size, and
17 the crystalline quality distribution in depth, expecting a preferential Si (111) orientation
18 on YSZ like the direct deposition case^{12,13)}. Since it lies beyond the scope of this paper,
19 this will be discussed in future work in more detail.

20 The open circles in Fig. 3 indicate that preheating shortens τ_i by ~ 250 min as
21 compared to the non-preheating case of the Si/poly-YSZ/glass. This suggests that
22 thermal heating in the vacuum chamber should be effective to promote Si nucleation.
23 But the crystallization rate $R_C = \Delta X_c / \Delta t_a$ is almost the same as in the non-preheating case,
24 which indicates that preheating hardly enhances R_C . So, we should notice that no matter

1 how much the interface property is improved, R_C is hardly changed although τ_i is
2 shortened.

3 Figure 4 shows Arrhenius plots of the reciprocal of the incubation time $1/\tau_i$ of the
4 three kinds of samples without preheating, the $1/\tau_i$ of Si/poly-YSZ/glass samples with
5 preheating, and crystalline fraction rates R_C of Si/(111)-YSZ and Si/poly-YSZ/glass
6 samples without preheating, with respect to the reciprocal of the annealing temperature
7 T_A . The solid and broken lines for the data of each sample group indicate calculation
8 results by the least square method. The R_C of the Si/glass sample is not shown because it
9 is hardly determined due to the non-linear curve shown in Fig. 3. As one can see, each
10 physical quantity exhibits the behavior of an activation process, and $1/\tau_i$ can be
11 formulated by $C_i \exp(-E_i/kT)$, where C_i and E_i are a pre-exponential factor and an
12 activation energy, respectively. The E_i s for the Si/(111)-YSZ, the Si/poly-YSZ/glass,
13 and the Si/glass are estimated to be about 4.3, 4.0, and 3.9 eV, respectively. The
14 activation energy E_{ip} for Si/poly-YSZ/glass with preheating is about 3.4 eV, and the
15 activation energies E_C of R_C for the Si/(111)-YSZ and the Si/poly-YSZ/glass are about
16 3.4 eV. The estimation error for them is less than 15 % roughly. The E_i s of the three
17 samples without preheating are similar within the error and are reduced by preheating.
18 Also, the estimated E_C is similar to the reported values of 3.1 to 3.4 eV.^{21, 24)}

19 Here, we will discuss the results of Fig. 4. According to the previous review
20 paper,²⁴⁾ it can be hypothesized that $1/\tau_i$ is proportional to a product of the nucleation
21 site area density $S_n(T) = S_{n0} \exp(-E_S/kT)$ and the Si atomic jump frequency
22 $\nu(T) = \nu_0 \exp(-E_V/kT)$ from amorphous phase to crystalline phase, as shown in the
23 following eq. (1). S_{n0} and ν_0 are pre-exponential factors of $S_n(T)$ and $\nu(T)$, respectively,
24 and E_S and E_V are activation energies of $S_n(T)$ and $\nu(T)$, respectively. So, C_i and E_i are

1 proportional to $S_{no} \cdot \nu_0$ and equal to $E_S + E_V$, respectively:

$$2 \quad \frac{1}{\tau_i} = C_i \exp\left(-\frac{E_i}{kT}\right) \propto S_n(T) \nu(T) = S_{no} \nu_0 \exp\left(-\frac{E_S + E_V}{kT}\right) . \quad (1)$$

3 In the comparison between bulk nucleation (BN) and interface nucleation (IN), the S_n of
4 IN is larger than that of BN, since IN generally occurs more often, as mentioned before.

5 Also, since ν depends mainly on the crystalline material, structure, and on the
6 temperature, each ν for the three kinds of samples can be the almost same. Furthermore,
7 it has been reported that, in the case of BN, E_C is roughly equal to $E_i^{21,24)}$ because both
8 E_C and E_i strongly depend on Si atomic jumping between the amorphous-crystalline
9 interface.

10 Based on these considerations, from the result of a τ_i of the Si/glass that is larger
11 than that of the Si on YSZ, we can conclude that the former pre-exponential factor of S_n
12 is smaller than that of the latter because their ν are almost the same. Also, it seems
13 reasonable that the E_i s of the three samples without preheating are roughly equal if it is
14 hypothesized that the difference in E_S is much smaller among the three samples,
15 compared with E_V . Furthermore, we can explain the reason why, by preheating, the E_i of
16 the Si/poly-YSZ/glass is reduced to E_{ip} and becomes close to the E_C of the growth rate
17 as follows: the interface of the YSZ without preheating has some contaminations or
18 chemical unstable sites, which may easily react with Si to prevent Si movement. This
19 may increase the E_S of S_n . By preheating, the obstacles are roughly removed, so that the
20 E_S is reduced. Therefore, $E_i = E_S + E_V$ is reduced and the E_{ip} becomes close to the E_C of
21 the crystallization growth rate.

22 There are still two questions concerning Figs. 3 and 4. The first one is that the τ_i
23 for the Si/(111)-YSZ is almost equal to that for the Si/poly-YSZ/glass. It is supposed
24 that the interface quality of the single (111)-YSZ must be much higher than that of the

1 poly-YSZ layer, so that the (111)-YSZ should have a shorter τ_i than the poly-YSZ. The
2 second question is why the S_n of Si on YSZ is larger than that for the Si/glass. To
3 answer these questions, as a possible cause, we may think of the Zr and Y of the
4 constituent elements of YSZ. From the concentration depth profiles of Zr and Y in the
5 crystallized Si film on the poly-YSZ layer obtained by SIMS, where $t_a = 1320$ min and
6 the preheating time = 60 min, it was found that Zr atoms diffuse into the crystallized
7 film at a level of less than 1×10^{18} atoms/cm³, and that the Y signal is near 1×10^{16}
8 atoms/cm³. From this result, this unignorable Zr concentration can be considered to be
9 one possible factor for the larger S_n irrespective of the interface crystalline quality. An
10 interaction of the free electrons of Zr with the covalent electrons of a nearest neighbor
11 Si might promote nucleation or bonding between Si atoms.²⁵⁾ On the other hand, it can
12 be said that, for crystallization growth in the film bulk, the diffusion of Zr and Y is a
13 negligible effect. This is not only because the SPC rate of about 50 nm/h shown in Fig.
14 2 is much lower than the MILC rates of more than 4 $\mu\text{m/h}$ that is the popular reported
15 value,²⁶⁾ but also because the impurity concentration level for Ni-MILC is greater than
16 ~ 0.08 at% ($\sim 4 \times 10^{19}$ atoms/cm³),⁶⁾ which is much larger than in our case by 1.5 orders
17 of magnitude. However, its effect on the electrical property for device application is to
18 be taken into account so that we should investigate the electrical property of the
19 crystallized Si film in future research.

20 In conclusion, we investigated the CI effect of YSZ in the solid phase crystallization
21 of a-Si film by using three kinds of samples, which were a-Si film/poly-YSZ/glass, a-Si
22 film/(111)-YSZ substrate, and a-Si film/glass. It was found that the τ_i of the poly-YSZ
23 layer was shorter than that for the glass substrate, and was almost equal to that for the
24 crystal (111) YSZ substrate. From the results of the Arrhenius plots of $1/\tau_i$, it was

1 deduced that the CI effect was not due to difference in E_i but to a higher S_n on YSZ,
2 because the E_i s of the three kinds of samples are similar. One possible factor for the
3 higher S_n can be considered to be Zr, which is one component of YSZ. It was also found
4 that the preheating prior to Si film deposition was effective in shortening τ_i . This is
5 probably because the preheating reduces E_i from about 4.0 eV to about $E_{ip} = 3.4$ eV.
6

1 **References**

- 2 1) A. Mimura, N. Konishi, K. Ono, J.-I. Ohwada, Y. Hosokawa, Y. A. Ono, T. Suzuki, K.
3 Miyata, and H. Kawakami, IEEE Trans. Electron Devices **36**, 351(1989).
- 4 2) J. N. Lee, Y. W. Choi, B. J. Lee, and B. T. Ahn, J. Appl. Phys. **82**, 2918(1997).
- 5 3) S. F. Gong, H. T. G. Hentzell, A. E. Robertsson, L. Hultman, S.-E. Hörnström, and G.
6 Radnoczi, J. Appl. Phys. **62**, 3726(1987).
- 7 4) Z. Jin, G. A. Bhat, M. Yeung, H. S. Kwok, and M. Wong, J. Appl. Phys. **84**,
8 194(1998).
- 9 5) S.-W. Lee, Y.-C. Jeon, and S.-K. Joo, Appl. Phys. Lett. **66**, 1671(1995).
- 10 6) M. Wang and M. Wong, IEEE Trans. Electron Devices **48**, 1655(2001).
- 11 7) T. Sameshima, M. Hara, and S. Usui, Jpn. J. Appl. Phys. **28**, L2131(1989).
- 12 8) S. Horita, Y. Nakata, and A. Shimoyama, Appl. Phys. Lett. **78**, 2250(2001).
- 13 9) S. Horita, H. Kaki, and K. Nishioka, Jpn. J. Appl. Phys. **46**, 3527(2007).
- 14 10) J. S. Im and H. A. Atwater, Appl. Phys. Lett. **57**, 1766(1990).
- 15 11) P. Reinig, F. Fenske, W. Fuhs, A. Schöpke, and B. Selle, Appl. Surf. Sci. **210**,
16 301(2003).
- 17 12) Horita and H. Sukreen, Appl. Phys. Express **2**, 041201(2009).
- 18 13) S. Horita and S. Hana, Jpn. J. Appl. Phys. **49**, 105801(2010).
- 19 14) S. Hana, K. Nishioka, and S. Horita, Thin Solid Films **517**, 5830(2009).
- 20 15) T. Kaneko, M. Wakagi, K. Onisawa, and T. Minemura, Appl. Phys. Lett. **64**,
21 1865(1994).
- 22 16) E. A. T. Dirani, A. M. Andrade, L. K. Noda, F. J. Fonseca, and P. S. Santos, J.
23 Non-Cryst. Solids **273**, 307(2000).
- 24 17) L. Haji, P. Joubert, M. Guendouz, N. Duhamel, and B. Loisel, MRS Proc. **230**,

- 1 177(1992).
- 2 18) J. N. Lee, B. J. Lee, D. G. Moon, and B. T. Ahn, *Jpn. J. Appl. Phys.* **36**, 6862(1997).
- 3 19) K. N. Tu, J. W. Mayer, and L. C. Feldman, *Electronic Thin Film Science for*
4 *Electrical Engineers and Materials Scientists* (Macmillan, New York, 1992) Chap.
5 10, pp. 256-262.
- 6 20) R. Bisaro, N. Proust, J. Magariño, and K. Zellama, *Thin Solid Films* **124**,
7 171(1985).
- 8 21) R. Bisaro, J. Magariño, Y. Pastol, P. Germain, and K. Zellama, *Phys. Rev. B* **40**,
9 7655(1989).
- 10 22) E. Bustarret, M. A. Hachicha, and M. Brunel, *Appl. Phys. Lett.* **52**, 1675(1988).
- 11 23) D. Han, G. Yue, J. D. Lorentzen, J. Lin, H. Habuchi, and Q. Wang, *J. Appl. Phys.* **87**,
12 1882(2000).
- 13 24) C. Spinella, S. Lombardo, and F. Priolo, *J. Appl. Phys.* **84**, 5383(1998).
- 14 25) K. N. Tu, *Appl. Phys. Lett.* **27**, 221(1975).
- 15 26) J. Jang: in *Thin Film Transistors: Materials and Processes*, ed. Y. Kuo (Kluwer,
16 Dordrecht, 2004) Vol. 2, p. 246.
- 17

1 Figure captions

2

3 Fig. 1 (Color online) Schematic diagrams of the three kinds of sample structures. (a)
4 a-Si film deposited on a poly-YSZ film which covers the surface of a fused quartz
5 substrate (Si/poly-YSZ/glass), (b) a-Si film deposited on a single crystal (111)-oriented
6 YSZ substrate (Si/(111)-YSZ), and (c) a-Si film deposited on a fused quartz substrate
7 (Si/glass).

8

9 Fig. 2 Raman spectra for the samples of the (a) Si/poly-YSZ/glass, (b) Si/(111)-YSZ,
10 and (c) Si/glass. The annealing temperature T_A is 560°C and the annealing time t_a is a
11 parameter.

12

13 Fig. 3 (Color online) Annealing time t_a dependencies of the crystalline fractions X_c of
14 Si films deposited on a poly-YSZ layer (closed circle), a single (111)-YSZ substrate
15 (cross), a glass substrate (closed triangle) without preheating, and on a preheated
16 poly-YSZ layer (open circle). As a reference, the broken line indicates the X_c of the Si
17 film annealed at 700 °C for 30 min on a single (111)-YSZ substrate without preheating.
18 The R_C of the crystalline fraction rate is defined by $\Delta X_c/\Delta t_a$ of the initial slope of the
19 linear line of the crystalline fraction versus t_a , and the τ_i of the incubation time is
20 determined by the intercepting time t_a between the horizontal axis and the linear line.

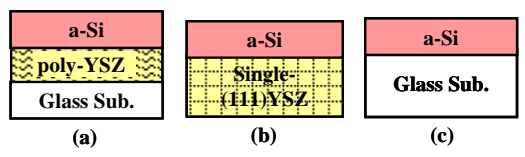
21

22 Fig. 4 (Color online) Arrhenius plots of the reciprocal of the incubation time $1/\tau_i$ and the
23 crystalline fraction rates R_C versus the reciprocal of the annealing temperature T_A . The
24 solid and broken lines for the data of each sample group are calculated by the least

1 square method.

2

1
2
3
4
5
6
7
8
9
10
11
12
13
14
15
16
17
18
19
20
21
22
23



24 **Fig. 1**

RC of JJAP, S. Horita et al.

1
2
3
4
5
6
7
8
9
10
11
12
13
14
15
16
17
18
19
20
21
22
23
24

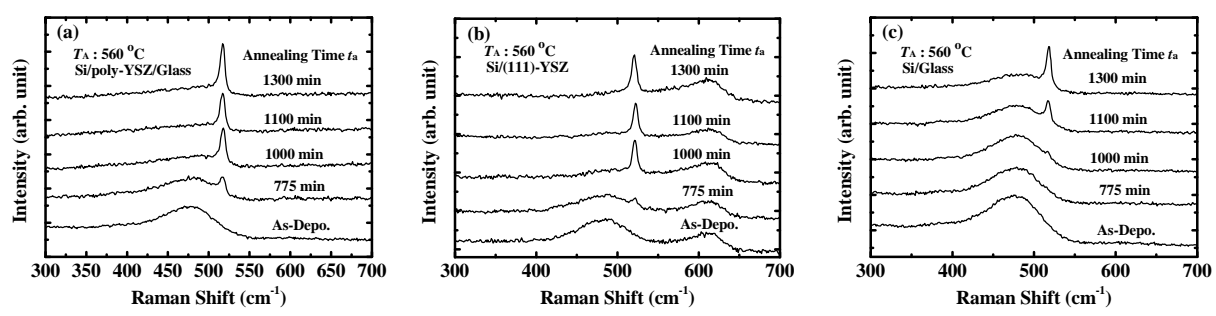


Fig. 2

RC of JJAP, S. Horita et al.

1
2
3
4
5
6
7
8
9
10
11
12
13
14
15
16
17
18
19
20
21
22
23
24

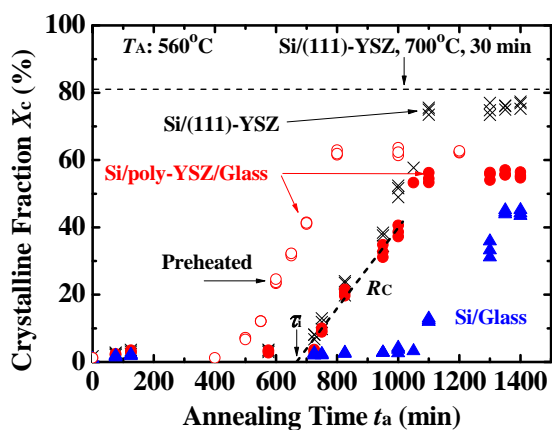


Fig. 3

RC of JJAP, S. Horita et al.

1
2
3
4
5
6
7
8
9
10
11
12
13
14
15
16
17
18
19
20
21
22
23
24

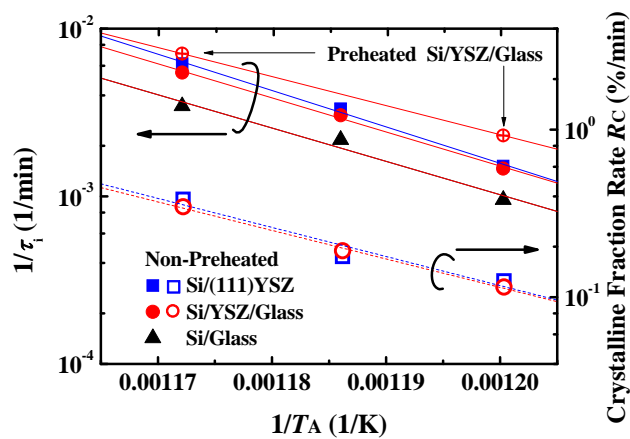


Fig. 4

RC of JJAP, S. Horita et al.